JB Journals.ASM.org

Biochemical and Biophysical Characterization of the Two Isoforms of *cbb*$_3$-Type Cytochrome *c* Oxidase from *Pseudomonas stutzeri*

Hao Xie,[a] Sabine Buschmann,[a] Julian D. Langer,[a] Bernd Ludwig,[b] Hartmut Michel[a]

Molecular Membrane Biology, Max Planck Institute of Biophysics, Frankfurt am Main, Germany[a]; Institute of Biochemistry, Molecular Genetics, Goethe University, Frankfurt am Main, Germany[b]

The *cbb*$_3$-type cytochrome *c* oxidases (*cbb*$_3$-C*c*Os) are members of the heme-copper oxidase superfamily that couple the reduction of oxygen to translocation of protons across the membrane. The *cbb*$_3$-C*c*Os are present only in bacteria and play a primary role in microaerobic respiration, being essential for nitrogen-fixing endosymbionts and for some human pathogens. As frequently observed in *Pseudomonads*, *Pseudomonas stutzeri* contains two independent *ccoNO*(*Q*)*P* operons encoding the two *cbb*$_3$ isoforms, Cbb$_3$-1 and Cbb$_3$-2. While the crystal structure of Cbb$_3$-1 from *P. stutzeri* was determined recently and *cbb*$_3$-C*c*Os from other organisms were characterized functionally, less emphasis has been placed on the isoform-specific differences between the *cbb*$_3$-C*c*Os. In this work, both isoforms were homologously expressed in *P. stutzeri* strains from which the genomic version of the respective operon was deleted. We purified both *cbb*$_3$ isoforms separately by affinity chromatography and increased the yield of Cbb$_3$-2 to a similar level as Cbb$_3$-1 by replacing its native promoter. Mass spectrometry, UV-visible (UV-Vis) spectroscopy, differential scanning calorimetry, as well as oxygen reductase and catalase activity measurements were employed to characterize both *cbb*$_3$ isoforms. Differences were found concerning the thermal stability and the presence of subunit CcoQ. However, no significant differences between the two isoforms were observed otherwise. Interestingly, a surprisingly high turnover of at least 2,000 electrons s^{-1} and a high Michaelis-Menten constant (K_m ~ 3.6 mM) using ascorbate–*N*,*N*,*N*′,*N*′-tetramethyl-*p*-phenylenediamine dihydrochloride (TMPD) as the electron donor were characteristic for both *P. stutzeri cbb*$_3$-C*c*Os. Our work provides the basis for further mutagenesis studies of each of the two *cbb*$_3$ isoforms specifically.

Heme-copper oxidases (HCOs), the terminal enzymes in the respiratory chain, are membrane-embedded proteins that catalyze the four-electron reduction of molecular oxygen to water, coupling this exothermic reaction to the establishment of a proton electrochemical gradient across the membrane bilayer (1–3). All HCOs share a transmembrane catalytic subunit, which contains a low-spin heme (*a* or *b*) and a binuclear center consisting of Cu$_B$ and a high-spin heme (a_3, b_3, or o_3). The HCO superfamily is phylogenetically subdivided into three major families: A, B, and C (4, 5). The A family HCOs, represented by the well-studied aa_3-type cytochrome *c* oxidases (aa_3-C*c*Os), are found in mitochondria and many bacteria. The B family of HCOs contains a number of bacterial and archaeal oxidases. In contrast, the C family is formed by the *cbb*$_3$-type cytochrome *c* oxidase (*cbb*$_3$-C*c*O) and is found only in bacteria. It remains less well characterized.

The *cbb*$_3$-C*c*Os, comprising more than 20% of the HCOs, are widely distributed within the bacterial phyla but particularly abundant in *Proteobacteria* (6–8). They have been studied in several Gram-negative bacteria (for recent reviews, see references 8 and 9). The *cbb*$_3$-C*c*Os were shown to be expressed predominantly under low oxygen tension (10) and are characterized by their high affinity for O_2 (11). Therefore, for instance, in the symbiotic diazotrophs, *cbb*$_3$-C*c*Os are needed to provide energy required for the ATP-consuming process of N_2 fixation and may serve to protect the oxygen-sensitive nitrogenase by oxygen scavenging (12). In some human pathogens, e.g., *Helicobacter pylori* (13) and *Neisseria meningitidis* (14), the *cbb*$_3$-C*c*O is the only respiratory oxidase encoded by the genome and is believed to be crucial for the colonization of the hosts under hypoxic conditions (8). In addition to the reduction of molecular oxygen, *cbb*$_3$-C*c*Os, which are structurally and phylogenetically related to bacterial nitric oxide reductases (NORs) (6, 15), were shown to reduce NO (16, 17) with a higher turnover number than oxidases from the A and B families (18).

The *cbb*$_3$-C*c*Os show a distinctly different subunit composition compared to A and B family HCOs as confirmed by the recently determined X-ray crystallographic structure (19). Typically, the *cbb*$_3$-C*c*Os are composed of CcoN, -O, -Q, and -P subunits, which were first identified as gene products of a *ccoNOQP* (*fixNOQP*) operon in the symbiotic N_2-fixing diazotrophs (20). The catalytic subunit CcoN of the *cbb*$_3$-C*c*Os is homologous to subunit I of the A family HCOs but has a very low sequence identity (less than 20%). It possesses 12 transmembrane helices and contains a low-spin heme *b* and a high-spin heme b_3-Cu$_B$ active center. Subunit CcoO possesses one transmembrane helix and a single C-type heme. Together with CcoN, it defines the core complex, because only these two subunits are observed in all *cbb*$_3$-C*c*Os (6) and can form assembly intermediates after insertion into the membrane (9, 21, 22). In alpha-, beta-, gamma-, and epsilonproteobacteria as well as in the *Aquificales*, a third subunit, CcoP (6), is found that possesses two transmembrane helices and two C-type hemes. Based on structural features, CcoP was proposed to be the initial electron acceptor receiving electrons from a periplasmic cytochrome *c* (19). It has also been suggested to serve as a gas-sensing

Received 10 September 2013 **Accepted** 5 November 2013
Published ahead of print 8 November 2013
Address correspondence to Hartmut Michel, Hartmut.Michel@biophys.mpg.de.
Supplemental material for this article may be found at http://dx.doi.org/10.1128/JB.01072-13.

doi:10.1128/JB.01072-13

TABLE 1 *P. stutzeri* strains and plasmids used in this study

Strain or plasmid	Features and relevant phenotype	Reference
P. stutzeri strains		
ZoBell	Wild type, ATCC 14405	57
ΔCbb_3-1 mutant	ZoBell Δ*ccoNOP*-1::Kan^r	This study
ΔCbb_3-2 mutant	ZoBell Δ*ccoNOQP*-2::Kan^r	This study
Plasmids		
pEGFP-N1	Plasmid containing the EGFP gene, Kan^r	Clontech
pACYC184	Plasmid containing the p15A origin, Cam^r Tet^r	NEB
pJET1.2	Blunt cloning plasmid	Fermentas
pBBR1MCS	Broad-host-range, low-copy-no. plasmid, Cam^r	58
pBBR1MCS-2	pBBR1MCS derivative, Kan^r	59
pBBR1MCS-2-EGFP	pBBR1MCS-2 derivative, EGFP gene	This study
pXH-B	Suicide plasmid, EGFP gene, p15A origin, Kan^r	This study
pXH-Δ1	pXH-B derivative, homologous flanking arms H1 and H2	This study
pXH-Δ2	pXH-B derivative, homologous flanking arms H2 and H3	This study
pXH-22	*P. stutzeri ccoNOP*-1 cloned into pBBR1MCS, Strep tag II at the C terminus of *ccoN*-1	This study
pXH-26	*P. stutzeri ccoNOQP*-2 cloned into pBBR1MCS, Strep tag II at the C terminus of *ccoN*-2	This study
pXH-39	pXH-26 derivative, promoter of *ccoNOQP*-2 replaced with promoter of *ccoNOP*-1	This study

element because one reduced heme *c* in this subunit can bind carbon monoxide (8). CcoQ is the smallest subunit present in some cbb_3-C*c*Os, which was shown to be involved in the stabilization of the cbb_3-C*c*O by interaction with subunit CcoP in *Rhodobacter capsulatus* (23) and by protection of the cbb_3-C*c*O from oxidative destabilization in *Rhodobacter sphaeroides* (24).

In the present work, we focus on the cbb_3-C*c*O of *Pseudomonas stutzeri*, a Gram-negative bacterium widely distributed in aquatic and terrestrial habitats (25), which possesses a branched respiratory chain that allows adaption to various environmental conditions. Earlier, *P. stutzeri* strain ZoBell was reported to possess only one *ccoNOQP* operon coding for cbb_3-C*c*O (26). More recently, we showed that this strain actually possesses two independent cbb_3 operons, encoding isoforms of cbb_3-C*c*O as well as Cbb_3-1 and Cbb_3-2 (19) (GenBank accession number HM130676). The presence of two cbb_3 operons was confirmed by the recently published draft genome sequence of *P. stutzeri* ZoBell (27). Although the plant pathogen *Pseudomonas syringae* possesses only one cbb_3-C*c*O, the presence of two cbb_3 operons is commonly found in the genus *Pseudomonas*, for example, in the opportunistic human pathogens *Pseudomonas aeruginosa* and *Pseudomonas putida* (7, 28). Previous studies on differential expression of Cbb_3-1 and Cbb_3-2 from *P. aeruginosa* indicated that the two isoforms differ from each other in their regulatory properties under different oxygen tensions (28, 29). However, the relevant functional differences between two isoforms of cbb_3-C*c*O are not known.

In *P. stutzeri*, both cbb_3 operons contain the three structural genes for the subunits CcoN, CcoO, and CcoP, whereas the gene *ccoQ* is present only in the second cbb_3 operon (*ccoNOQP*-2). A DNA sequence comparison showed that the first cbb_3 operon (*ccoNOP*-1) has, on average, a 79% identity with *ccoNOQP*-2, which might explain why only one operon was found previously (26). The amino acid sequence identities of the two cbb_3 isoforms are also very high, 87% for subunit CcoN, 97% for subunit CcoO, and 63% for subunit CcoP. Due to the high homology between Cbb_3-1 and Cbb_3-2, both isoforms are usually found as a mixture in the same chromatographic fractions during the purification process. Although the separation of both cbb_3-C*c*Os is difficult, the wild-type Cbb_3-1 was successfully purified to homogeneity from the native membranes of *P. stutzeri* by four conventional chromatographic steps, and its structure was determined by X-ray crystallography (19). However, we could not isolate isoform Cbb_3-2 from the protein mixture using the same purification strategy. To overcome this difficulty, we established a homologous expression system, including two *P. stutzeri* deletion stains and the use of an expression vector. Two recombinant cbb_3 isoforms are produced from the corresponding *P. stutzeri* deletion strains and purified separately by applying affinity chromatography. Here we report the biochemical and biophysical characterization of two separated isoforms of cbb_3-C*c*O from *P. stutzeri*, and a rigid discrimination is now available.

MATERIALS AND METHODS

Bacterial strains, plasmids, oligonucleotides, and media. The bacterial strains and plasmids used in this study are listed in Table 1. Synthetic oligonucleotides, obtained from Eurofins MWG Operon (Ebersberg, Germany), are listed in Table S1 in the supplemental material. *Pseudomonas stutzeri* strain ZoBell (ATCC 14405) was used throughout the present work. Two *P. stutzeri* cbb_3 deletion strains constructed in this study, namely, ΔCbb_3-1 and ΔCbb_3-2, were used for homologous expression of both recombinant isoforms of cbb_3-C*c*O. The *P. stutzeri* strains were grown on lysogeny broth agar or in asparagine minimal medium (30) with slight modifications concerning the supplementation of trace elements (32 mg $FeCl_3 \cdot 6H_2O$, 0.17 mg $CuCl_2 \cdot 2H_2O$, 1.6 mg NH_4NO_3, 22 mg KBr, 20 mg $MnCl_2 \cdot 2H_2O$, 25 mg $ZnCl_2$ per liter). Antibiotics were used at the following concentrations: 50 μg/ml kanamycin (Kan) and 68 μg/ml chloramphenicol (Cam) for both deletion strains containing the expression vector. *Escherichia coli* strains DH5α and JM110 were used for general cloning.

Construction of the cbb_3 deletion strains. To delete each of two chromosomal cbb_3 operons (*ccoNOP*-1 and *ccoNOQP*-2) by homologous recombination, suicide vectors that facilitate the selection of double-crossover events were constructed. A 751-bp BamHI-XbaI fragment from pEGFP-N1 was ligated into pBBR1MCS-2 digested by the same enzymes, resulting in pBBR1MCS-2–enhanced green fluorescent protein (EGFP), in which the EGFP gene product can serve as a reporter protein for allelic replacement. To introduce a suicide replicon into pBBR1MCS-2–EGFP, a 2.6-kb fragment containing the pBBR1 replicon and mobilization (mob) gene was replaced by the p15A replicon from pACYC184, yielding the plasmid pXH-B. Subsequently, the kanamycin resistance cassette of

pXH-B was flanked by the H1 fragment (−532 to +1 bp upstream of the translation start of *ccoN*-1) and the H2 fragment (−57 to +448 bp of the stop codon of *ccoP*-1) as 5′ and 3′ homologous regions, resulting in pXH-Δ1. Correspondingly, the same cassette was flanked at the 5′ end by the H2 fragment and at the 3′ end by the H3 fragment (−365 to +100 bp of the stop codon of *ccoP*-2), yielding the vector pXH-Δ2. A schematic representation of the construction of both suicide vectors is shown in Fig. S1 in the supplemental material. Both suicide vectors pXH-Δ1 and pXH-Δ2 were electrotransformed (31) individually into *P. stutzeri* ZoBell cells. The double-crossover event was selected for by an EGFP-negative and kanamycin-resistant phenotype. Substitution of the desired cbb_3 operons with the kanamycin resistance cassette was accomplished by comparing the PCR products from the wild-type and deletion strains and by direct sequencing (SeqLab, Göttingen, Germany).

Construction of the expression vectors. The genomic DNA of *P. stutzeri* ZoBell was isolated using the G-spin genomic extraction kit (iNtRON; Biotechnology, South Korea). Two DNA fragments containing the operon *ccoNOP*-1 (3,932 bp) and the operon *ccoNOQP*-2 (4,033 bp) with the corresponding promoter regions were amplified from the genomic DNA and cloned separately into pJET1.2 (Fermentas, St. Leon-Rot, Germany) for subcloning. For purification of the recombinant cbb_3-C*c*O by affinity chromatography, a Strep tag II was fused to the C terminus of *ccoN*-1 and *ccoN*-2 using the QuikChange site-directed mutagenesis kit (Agilent Technologies, Waldbronn, Germany). A 3.4-kb fragment containing Strep-tagged *ccoNOP*-1 was amplified, digested with the BamHI-HindIII endonucleases, and subcloned into the low-copy-number vector pBBR1MCS, resulting in pXH-22 (for the expression of Cbb_3-1). Likewise, a 3.6-kb fragment containing Strep-tagged *ccoNOQP*-2 was cloned into pBBR1MCS using ligation-independent cloning (In-Fusion cloning kit; Clontech, Mountain View, CA, USA), yielding pXH-26 (for the expression of Cbb_3-2). To increase the yield of Cbb_3-2, the native promoter of *ccoNOQP*-2 in pXH26 was replaced with the endogenous promoter region of *ccoNOP*-1, resulting in plasmid pXH39 (for the high-yield expression of Cbb_3-2). The final constructs for homologous expression of both isoforms of Cbb_3-C*c*O were verified by sequencing and introduced by electroporation into the ΔCbb_3-1 and ΔCbb_3-2 deletion strains.

Purification of cbb_3-C*c*Os. *P. stutzeri* ZoBell cells were cultured under microaerobic conditions and harvested according to the previously published procedures (30). A typical yield was 6 to 10 g of wet cells per liter of asparagine minimal medium. Membrane preparation was performed as described previously (30) with an additional low-salt (50 mM NaCl) washing step. Membranes were solubilized with *n*-dodecyl-β-D-maltoside (DDM; Glycon, Luckenwalde, Germany) at a ratio of 2.5 mg detergent per milligram of membrane protein. Purification of the wild-type Cbb_3-1 was performed by four chromatographic steps as published previously (19). To purify the Strep-tagged recombinant cbb_3-C*c*Os, the solubilized membranes were supplied with 0.2 mg/ml avidin and loaded onto a Strep-Tactin Superflow high-capacity column (IBA, Göttingen, Germany), which was preequilibrated with 20 mM Tris-HCl (pH 7.5), 100 mM NaCl, 0.5 mM EDTA, 10% (vol/vol) glycerol, and 0.02% (wt/vol) DDM, at a flow rate of 0.2 to 0.5 ml/min. The unusually low flow rate was necessary to allow sufficient binding of the recombinant cbb_3-C*c*Os to the column. The bound proteins were eluted with 5 mM desthiobiotin in equilibrium buffer and applied directly onto a Q Sepharose high-performance anion exchange column (GE Healthcare, Munich, Germany) at a flow rate of 2 ml/min. The cbb_3-C*c*O was eluted with a step of 300 mM NaCl in equilibration buffer and concentrated using Amicon concentrators with 100-kDa-cutoff membranes (Millipore, Billerica, MA, USA). During this concentration step, the concentration of NaCl in the buffer was reduced to 100 mM. Concentrated proteins were then loaded onto a Superdex 200 10/300 GL gel filtration column (GE Healthcare) at a flow rate of 0.5 ml/min. The elution profile was monitored at 280 nm and 411 nm, and the eluted protein fractions containing cbb_3-C*c*O were collected, concentrated to a final concentration of 100 to 200 μM, and flash frozen in liquid nitrogen for storage at −80°C.

SDS-PAGE, BN-PAGE, and heme staining. The purified cbb_3-C*c*Os were analyzed on self-cast 15% Tris-glycine SDS-PAGE gels (32) and stained with Coomassie brilliant blue. Heme staining was used to detect the heme-associated peroxidase activity of cbb_3-C*c*O subunits (33). Blue native (BN)-PAGE (34) was performed on 4 to 16% Bis-Tris gels according to the manufacturer's instructions (Novex, Life Technologies, Darmstadt, Germany).

Mass spectrometry. Peptide mass fingerprinting was performed as previously described (19). Briefly, the chemically modified proteins were subjected to proteolytic digestion using a combination of trypsin and chymotrypsin to increase the cleavage efficiency of both hydrophobic and hydrophilic domains. The proteolytic digests were analyzed by coupling a nano high-performance liquid chromatograph (nano-HPLC) (EASY-nLC; Proxeon, Odende, Denmark) to a quadrupole time of flight (TOF) mass spectrometer (maXis; Bruker Daltonics, Bremen, Germany) using a Bruker Apollo electrospray ionization (ESI) source with a nanoSprayer emitter or a chip-based nano-ESI source (TriVersa NanoMate; Advion, Ithaca, NY, USA). When applicable, the obtained peptides from nano-HPLC were simultaneously loaded onto a 384 AnchorChip matrix-assisted laser desorption ionization (MALDI) target (Bruker Daltonics) and subsequently analyzed using MALDI-TOF/TOF mass spectrometry (Autoflex III Smartbeam; Bruker Daltonics). Spectra were internally recalibrated on autoproteolytic trypsin fragments when applicable. Proteins were identified by matching the derived mass lists against the NCBI nonredundant protein database or a custom *Pseudomonas* database on a local Mascot server.

UV-visible spectrophotometry. UV-visible (UV-Vis) spectra of the purified cbb_3-C*c*Os were recorded on a Lambda 35 UV-Vis spectrometer (PerkinElmer, Waltham, MA, USA). Spectra of cbb_3-C*c*Os (0.8 to 2.0 μM) were measured between 380 nm and 640 nm in 20 mM Tris-HCl (pH 7.5), 100 mM NaCl, 50 μM EDTA, and 0.02% (wt/vol) DDM. Cbb_3-C*c*Os were oxidized with 10-fold molar excess of potassium hexacyanoferrate(III) and fully reduced by adding a small amount of sodium dithionite. The concentrations of oxidized cbb_3-C*c*Os were calculated using a molar extinction coefficient of $5.85 \times 10^5\ M^{-1}\ cm^{-1}$ at 411 nm (26).

Differential scanning calorimetry. Differential scanning calorimetry (DSC) was used to characterize the thermophysical properties of the cbb_3-C*c*Os. Measurements were performed on a Microcal VP-DSC capillary cell microcalorimeter (GE Healthcare). All sample and reference solutions were degassed at 4°C prior to use. Scans of protein samples (3.5 mg/ml cbb_3-C*c*O in 20 mM Tris-HCl [pH 7.5], 100 mM NaCl, 0.02% [wt/vol] DDM) were carried out from 10 to 120°C, at a scan rate of 90°C/hour with a 10-s filtering period in the low-feedback mode. All data were normalized and analyzed with the software supplied by the manufacturer. Thermophysical parameters (e.g., midpoint temperature [T_m] and enthalpy change [ΔH]) were further validated using a Gaussian function in Origin 8.6 software (Additive, Friedrichsdorf, Germany).

Polarographic oxygen measurements. The oxygen reductase activity of cbb_3-C*c*O was determined polarographically using a Clark-type oxygen electrode (OX-MR; Unisense, Aarhus, Denmark) connected to a picoammeter (PA2000 Multimeter; Unisense). The analog signals were converted into digital signals using an A/D converter (ADC-216; Unisense) and then recorded with the software Sensor Trace Basic 2.1 supplied by the manufacturer. Oxygen consumption was measured in 2-ml glass vials with stirring in a water bath at room temperature. The reaction vial was filled with 50 mM Tris-HCl (pH 7.5), 100 mM NaCl, 50 μM EDTA, and 0.02% (wt/vol) DDM, followed by the addition of 3 mM sodium ascorbate and 1 mM *N*,*N*,*N*′,*N*′-tetramethyl-*p*-phenylenediamine dihydrochloride (TMPD) to a final volume of 600 μl. The reaction was then initiated by adding 5 pmol of the cbb_3-C*c*O. The reaction was inhibited by the addition of 1 mM potassium cyanide. In this study, the dependence of oxygen reduction activity on pH and ionic strength was measured by varying the pH from 5.8 to 8.7 and the concentration of NaCl from 0 to 500 mM, respectively. The measurements were also performed with different con-

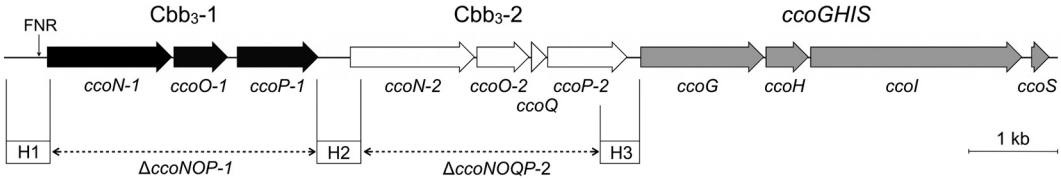

FIG 1 Schematic representation of the organization of the two cbb_3 operons and the *ccoGHIS* gene cluster on the *P. stutzeri* ZoBell chromosome. Genes are denoted by arrowheads according to their encoded products. cbb_3 operon *ccoNOP*-1 and *ccoNOPQ*-2 are shown in black and white, respectively. The *ccoGHIS* gene cluster (in gray) is located downstream of *ccoNOQP*-2 and is important for the assembly of the cbb_3-C*c*Os. The FNR box is found in the upstream region of *ccoN*-1. Three homologous regions (H1, H2, and H3) used for recombination are shown in boxes. The regions deleted and replaced with a kanamycin gene in deletion strains lacking Cbb_3-1 and Cbb_3-2 are indicated as dashed lines. Length standard (1 kb) is shown on the right.

centrations of TMPD (0.5 to 4.0 mM) and with different molar ratios of ascorbate to TMPD.

To compare the catalase activity between the wild-type Cbb_3-1 and recombinant Cbb_3-1 and Cbb_3-2, oxygen production was measured as previously described (35). Briefly, hydrogen peroxide was added to the buffer mentioned above to a final concentration of 600 μM, and the reaction was initiated by adding cbb_3-C*c*O to a final concentration of 500 nM. The catalase activity is presented as turnover number per minute (O_2 produced per minute per cbb_3-C*c*O). The steady-state activity of cbb_3-C*c*O was determined from the slope within 10 s after the reaction initiation. Data processing and analyses were performed with the software Origin 8.6 (Additive).

RESULTS

Organization of the two cbb_3 operons and the construction of deletion strains. A 12-kb genomic DNA fragment, possessing two cbb_3 operons (*ccoNOP*-1 and *ccoNOQP*-2) and a *ccoGHIS* gene cluster, was identified in the genome of *P. stutzeri* ZoBell (Fig. 1). The numbering order of the two cbb_3 operons is based on the genome annotation of *P. stutzeri* strain A1501 (36). Each of the two cbb_3 operons, separated by a 352-bp segment, encodes the subunits of two isoforms of cbb_3-C*c*O, namely, Cbb_3-1 and Cbb_3-2. Both operons contain the genes for CcoN, CcoO, and CcoP, while the *ccoQ* gene is found only in *ccoNOQP*-2. A consensus arginine nitrate regulation (ANR), or fumarate and nitrate reduction regulator (FNR), binding motif (TTGAT-N^4-gTCAA) is located directly upstream of the *ccoN*-1 transcription start site. The *ccoGHIS* cluster, located 137 bp downstream of *ccoNOQP*-2, is required for the maturation and assembly of a functional cbb_3-C*c*O (9).

For a detailed comparison of both isoforms, we constructed two deletion strains using the strategy of homologous recombination, which requires three long homology arms (H1, H2, and H3, ~500 bp) (Fig. 1). The two strains contain a disruption in the loci encoding Cbb_3-1 (Δ*ccoNOP*-1) and Cbb_3-2 (Δ*ccoNOQP*-2), respectively. Substitution of the *ccoNO*(*Q*)*P* operon with the kanamycin resistance cassette and verification of gene deletion were accomplished by PCR analysis and by direct resequencing of the selected 12-kb genomic regions.

Both recombinant cbb_3 isoforms are separately expressed and isolated. To isolate both recombinant cbb_3 isoforms, two cbb_3 operons with corresponding promoter regions were individually cloned into the broad-host-range vector pBBR1MCS. A Strep tag II was introduced at the C terminus of subunit CcoN, allowing the independent and specific purification of both cbb_3 isoforms by affinity chromatography. The expression vector pXH22, harboring the operon *ccoNOP*-1, was transformed into the ΔCbb_3-1 deletion strain to produce the recombinant Strep-tagged Cbb_3-1. Likewise, the expression vector pXH26 containing the operon *ccoNOQP*-2 was introduced into the ΔCbb_3-2 deletion strain to obtain the recombinant Cbb_3-2. Both homologously expressed recombinant cbb_3 isoforms were purified to homogeneity using three chromatographic steps as described in Materials and Methods. In this study, although the oxygen level was not controlled during the cultivation of both *P. stutzeri* recombinant strains, we found that the oxygen concentration in the culture was normally below 5 μM (≈3 mm Hg) after *P. stutzeri* cells had entered the exponential growth phase. Under this microaerobic condition, expression of Cbb_3-1 and Cbb_3-2 in deletion strains from which the genomic version has been deleted show different protein yields (Table 2). To increase the expression of Cbb_3-2, we replaced the native promoter region of Cbb_3-2 by the endogenous promoter of Cbb_3-1, resulting in pXH39. After the promoter exchange, the yield of Cbb_3-2 was increased 4- to 6-fold to 2 to 3 mg purified protein per liter of culture medium, which is comparable to the yield of Cbb_3-1 (Table 2).

We next analyzed both purified cbb_3 isoforms by SDS-PAGE. After Coomassie brilliant blue staining, three distinct bands with apparent molecular masses of 42, 36, and 24 kDa were visible (Fig. 2A), which correspond to subunits CcoN, CcoP, and CcoO of the cbb_3-C*c*O according to the results of our peptide mass fingerprinting analysis. This SDS-PAGE pattern is consistent with previous reports of the wild-type cbb_3-C*c*O (30). Due to the strong hydrophobic properties of CcoN and the binding of detergent, CcoN subunits of both cbb_3 isoforms migrated significantly faster than expected from their molecular masses (52.79 kDa for CcoN-1 and 53.17 kDa for CcoN-2). When SDS-PAGE gels were stained for heme-associated peroxidase activity in the presence of TMPZ and H_2O_2, we observed two major stained bands corresponding to the subunits CcoP and CcoO, since these two smaller subunits contain covalently bound heme C (Fig. 2B). Although the predicted masses of CcoP-1 (34.89 kDa) and CcoP-2 (35.01 kDa) are very similar, a difference in the migration distance has been noted, which allows to distinguish both cbb_3 isoforms. In contrast to subunit CcoP, however, the sizes of CcoO-1 (23.43 kDa) and CcoO-2 (23.46 kDa) are too close to show any difference. In addition, subunit CcoQ has a low molecular mass of 6.91 kDa and is

TABLE 2 Summary of the typical yield of recombinant cbb_3-C*c*Os

Expression vector	Isoform	Features of promoter	Yield (mg/liter)
pXH22	Cbb_3-1	Native promoter of *ccoNOP*-1 (P1)	2–4
pXH26	Cbb_3-2	Native promoter of *ccoNOQP*-2 (P2)	<0.5
pXH39	Cbb_3-2	Endogenous promoter of *ccoNOP*-1 (P1)	2–3

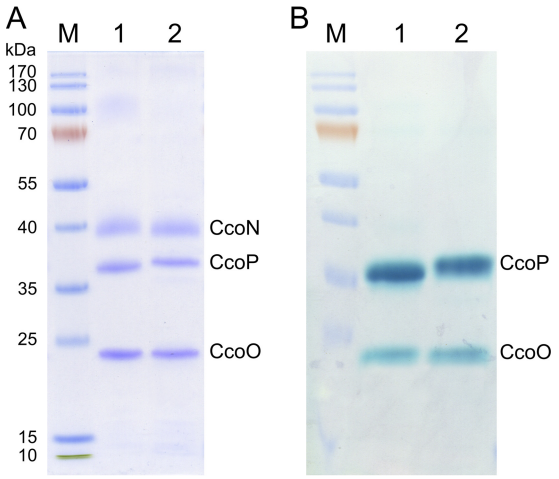

FIG 2 SDS-PAGE gels and heme staining of both purified recombinant *cbb*$_3$ isoforms. (A) A total of 10 μg each of the isolated recombinant Cbb$_3$-1 (lane 1) and Cbb$_3$-2 (lane 2) were separated on a Tris-glycine 15% SDS-PAGE gel and stained with Coomassie brilliant blue. (B) Gel stained for TMPZ mediated heme peroxidase activity. The molecular masses (in kDa) of the prestained protein standards (lane M) are shown on the left. Subunits CcoN, CcoP, and CcoO are indicated.

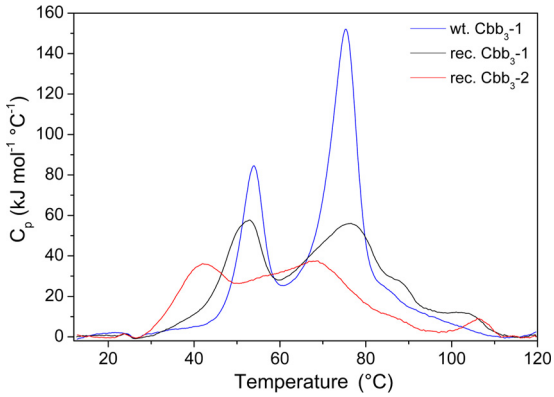

FIG 3 A comparison of thermal stability of wild-type Cbb$_3$-1 (blue line), recombinant Cbb$_3$-1 (black line), and recombinant Cbb$_3$-2 (red line). DSC profiles of oxidized (as isolated) *cbb*$_3$-C*c*Os (3.5 mg/ml) were obtained at a heating rate of 90°C/hour, and each curve was baseline subtracted.

stained poorly by the Coomassie dye. Furthermore, identification of CcoQ on this SDS-PAGE gel was not possible due to lack of detection of CcoQ by peptide mass fingerprinting.

Subunit composition of two *cbb*$_3$ isoforms is different. To evaluate the molecular mass and oligomeric state of both purified recombinant *cbb*$_3$-C*c*O complexes in their native state, protein samples were separated by BN-PAGE. Considering the mass contribution of bound heme ligands, the expected molecular masses of Cbb$_3$-1 and Cbb$_3$-2, based on the amino acid sequence of the monomeric form, are 112.3 and 119.8 kDa, respectively. When Cbb$_3$-1 and Cbb$_3$-2 were analyzed by BN-PAGE, we observed that both isoforms were resolved as a sharp single band with an apparent molecular mass of 165 kDa (see Fig. S2 in the supplemental material). Since the migration behavior of membrane proteins is strongly affected by the binding of lipids and detergents to the hydrophobic surface, our results from BN-PAGE still suggest that Cbb$_3$-1 and Cbb$_3$-2 are both present in a monomeric and monodisperse state under the current experimental conditions. To determine the subunit composition, protein bands in BN-PAGE were cut out and subsequently analyzed by peptide mass fingerprinting. Because both *cbb*$_3$ isoforms share a high sequence identity, the resulting peptide fragments were characterized by a coupling of nanoscale liquid chromatography-electrospray ionization-tandem mass spectrometry (NanoLC-ESI-MS/MS) and NanoLC-MALDI-MS/MS. The overall sequence coverages for each of the three subunits of Cbb$_3$-1 were 36.1% (CcoN-1), 74.5% (CcoO-1), and 66.6% (CcoP-1). A similar sequence coverage for Cbb$_3$-2 was observed, which was 31.9% (CcoN-2), 69.6% (CcoN-2), and 82.6% (CcoP-2). Even though the sequence coverage of subunit CcoN was low, the peptide mass fingerprinting analysis (see also Fig. S3 in the supplemental material) provided the following results. (i) Unique peptides from subunits CcoNOP of Cbb$_3$-1 and Cbb$_3$-2 were detected only in the corresponding isoforms. No chimeric proteins or fragments were found. (ii) The CcoQ subunit was observed only in Cbb$_3$-2, with a sequence coverage of 35.5%. (iii) The assembly protein CcoH was observed in both recombinant *cbb*$_3$-C*c*O complexes (see also Fig. S4 in the supplemental material). (iv) Besides CcoH, ribosomal proteins and histone-like DNA binding protein were also detected as general contaminants.

Both *cbb*$_3$ isoforms display very similar UV-Vis spectra. The room temperature electronic absorption spectra of fully oxidized, fully reduced, and reduced minus oxidized difference spectra of recombinant Cbb$_3$-1 and Cbb$_3$-2 are shown in Fig. S5 in the supplemental material. The spectra of wild-type Cbb$_3$-1 are not shown because they are identical with those obtained with recombinant Cbb$_3$-1. In the oxidized state, both *cbb*$_3$ isoforms contain an intense Soret maximum at 411 nm and two features at 529 and 559 nm. After reduction with dithionite, the Soret band was shifted to 418 nm and was increased in intensity. Two absorption maxima appeared at 521 and 552 nm, which are attributed to the ferrous forms of the C hemes. The reduction of both B hemes is accompanied by changes in two regions at 529 and 559 nm. Two slight differences between Cbb$_3$-1 and Cbb$_3$-2 were found in the alpha band of the reduced spectra. Cbb$_3$-2 has a maximum at 551.2 nm with a more intense shoulder at 559 nm, whereas the same maximum is red shifted to 551.8 nm with a less intense shoulder in Cbb$_3$-1. Furthermore, in the reduced minus oxidized difference spectra, one distinction occurs in the region of 420 to 440 nm, which indicates that the environment of heme *b* of the two *cbb*$_3$ isoforms reacts slightly differently upon reduction.

Both *cbb*$_3$ isoforms showed different thermal stability. In order to investigate the thermal stability of both *cbb*$_3$ isoforms, differential scanning calorimetry analyses were performed in the range between 10 and 120°C (Fig. 3). As a rescan of the same protein sample displayed no endothermic signal, this thermal denaturation was found to be irreversible, which is consistent with the results obtained from the yeast and *Paracoccus denitrificans* *aa*$_3$-C*c*Os (37, 38). Because of the irreversible nature of the thermal denaturation process, the calorimetric data cannot be directly analyzed in terms of equilibrium thermodynamics (39). Therefore, the calorimetric enthalpy change (ΔH) of thermal transition may not represent the true enthalpy change of unfolding. Nevertheless, the calorimetric enthalpy change can still be used to compare the thermal stability of the two *cbb*$_3$ isoforms.

With wild-type Cbb$_3$-1, two well-separated steps of tempera-

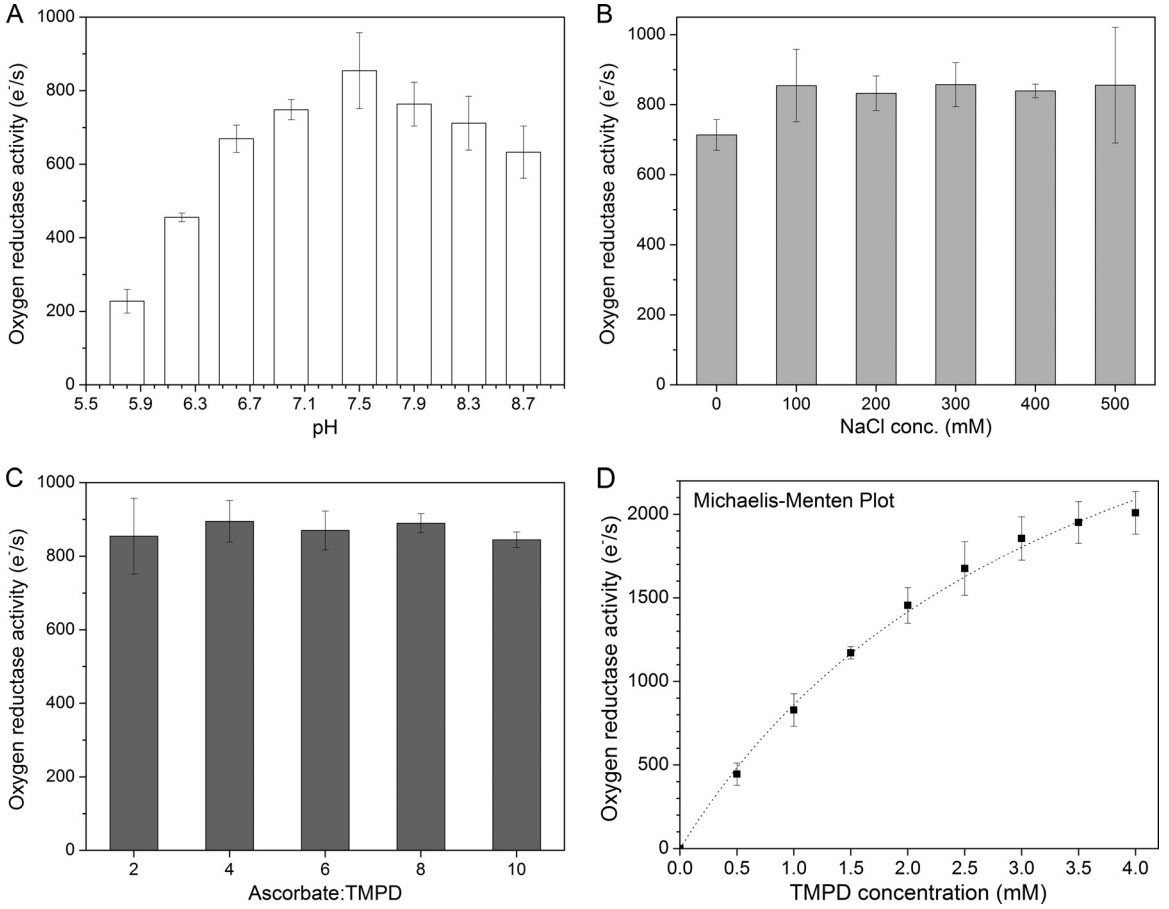

FIG 4 Oxygen reductase activity of wild-type Cbb_3-1 from *P. stutzeri* ZoBell. Each data point (turnover number) represents the mean value ± standard deviation (SD), which is calculated from at least five independent measurements. (A) pH dependence of the cbb_3-C*c*O activity was measured with 3 mM ascorbate, 1 mM TMPD, and 8.3 nM cbb_3-C*c*O by varying the pH from 5.8 to 8.7 and in the presence of 100 mM NaCl in the reaction buffer (50 mM Tris-HCl, 50 μM EDTA, 0.02% [wt/vol] DDM). The indicated pH was measured after the addition of ascorbate and TMPD, prior to the reaction initiation. (B) Dependence of the cbb_3-C*c*O activity on the concentration of NaCl (0 to 500 mM), measured under the same conditions as mentioned above, while maintaining the pH at 7.5. (C) Dependence of the cbb_3-C*c*O activity on the molar ratio of ascorbate to TMPD (2:1 to 10:1), measured in the presence of 100 mM NaCl at pH 7.5. (D) Dependence of the cbb_3-C*c*O activity on the concentration of TMPD. The dotted line shows a nonlinear regression fit of the experimental data according to the Michaelis-Menten equation.

ture-dependent transition were observed. Two T_m at 54.0 and 74.6°C are associated with an enthalpy change (ΔH) of 760 and 1,512 kJ mol^{-1}, respectively. The ratio of the enthalpy of the high-temperature to the low-temperature phase transition ($\Delta H_H/\Delta H_L$) is calculated to be 2. Compared to the wild-type Cbb_3-1, recombinant Cbb_3-1 shows two similar peaks centered at 51.2 and 75.0°C, whereas the latter has an enlarged shoulder at about 88°C. Although the intensity of both peaks is significantly decreased, the ΔH values change only slightly to 705 and 1,311 kJ mol^{-1} for the low- and high-temperature transitions, respectively, due to the broadening of the peaks. The $\Delta H_H/\Delta H_L$ ratio is 1.9, which is consistent with the observation from wild-type Cbb_3-1. In the case of recombinant Cbb_3-2, two transition peaks are apparently less well separated and less intense. The T_m of both peaks shifted to 41.4 and 65.1°C, indicating that the recombinant Cbb_3-2 denatures 10°C earlier than the recombinant Cbb_3-1. Moreover, ΔH_L and ΔH_H are correspondingly reduced to 402 and 1,154 kJ mol^{-1}, respectively, which confirms that recombinant Cbb_3-2 is less stable. The $\Delta H_H/\Delta H_L$ ratio of 2.9, as calculated for Cbb_3-2, is different from the observed ratio of Cbb_3-1.

Determination of the oxygen reductase activities and catalase activities. The cytochrome *c* oxidase activity of cbb_3-C*c*O was measured polarographically at 25°C using a Clark-type oxygen electrode. A combination of ascorbate and TMPD was used as the artificial respiratory substrate to study the oxygen reduction reaction. Oxygen consumption does not occur in the absence of cbb_3-C*c*O and can be completely inhibited by the addition of 1 mM KCN. To accurately measure the activity of cbb_3-C*c*O, we first optimized the reaction conditions by varying the pH, ionic strength, and ascorbate/TMPD ratio. Upon addition of various concentrations of ascorbate and TMPD, the pH value of the reaction system changes by approximately 0.1 to 0.5 units depending on the buffer composition. Therefore, we also tested three buffers (Tris, HEPES, and phosphate) for their effects on the enzyme activity assay. Tris buffer was chosen because this buffer gives the most sensitive results, and the pH was checked to verify that it was within ±0.05 units of the desired value during all the experiments. As shown in Fig. 4A, the cbb_3-C*c*O was found to be most active at pH 7.5, which is consistent with a previous report (26). By varying the concentration of NaCl in the range of 0 to 500 mM, the inter-

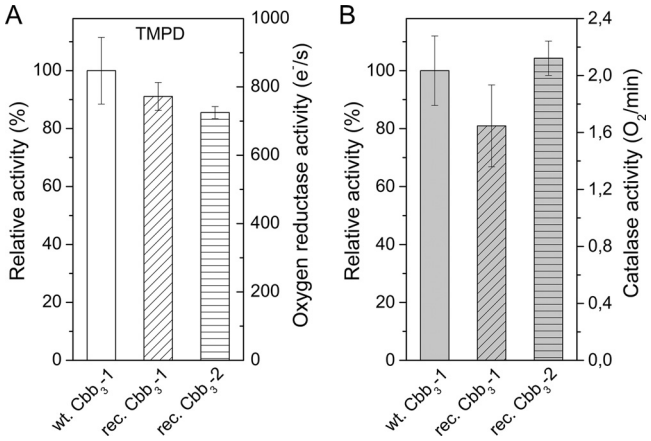

FIG 5 Comparison of the oxygen reductase activity and catalase activity between wild-type Cbb_3-1, recombinant Cbb_3-1, and Cbb_3-2. Each bar represents the mean value ± SD, calculated from at least five independent measurements. The relative activity was calculated by assuming that the activity observed from wild-type Cbb_3-1 was 100%. (A) Oxygen reductase activity was measured in the presence of 3 mM ascorbate, 1 mM TMPD, and 8.3 nM *cbb*$_3$-C*c*O at pH 7.5. (B) Catalase activity was measured in the presence of 600 μM hydrogen peroxide and 500 nM *cbb*$_3$-C*c*O.

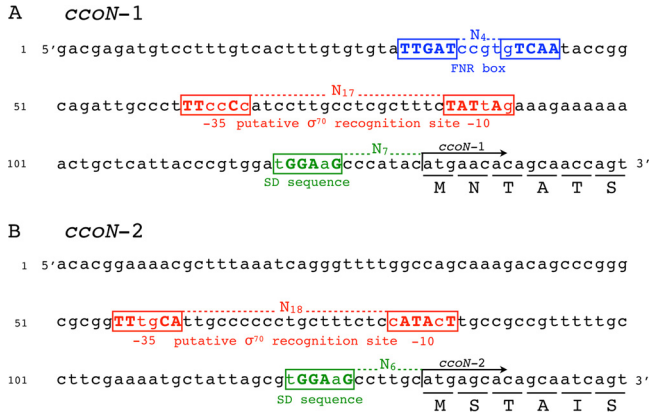

FIG 6 Nucleotide sequence (5′ to 3′) analysis of the upstream region of the *ccoN*-1 gene (A) and *ccoNOQP*-1 gene (B). An FNR (ANR) box (TTGAT-N^4-gTCAA) is located upstream of the *ccoN*-1 transcription start site and is shown in blue. Sequences in the red boxes exhibit homology to the −10 and −35 promoter regions recognized by the σ^{70}-containing RNA polymerase. The RpoD (σ^{70}) recognition site in panel A is proposed based on the previously identified data from *P. putida* (43). The potential Shine-Dalgarno sequence is shown in green. Conserved nucleotides (compared to the consensus sequences) are in bold and capitalized. The translation initiation sites are indicated by arrows. The first six amino acids are underlined.

action between TMPD and *cbb*$_3$-C*c*O appears to be independent of the ionic strength (Fig. 4B). Moreover, a molar ratio of 2:1 to 10:1 for ascorbate to TMPD showed no strong effect on the TMPD-mediated oxygen reductase activity of *cbb*$_3$-C*c*O (Fig. 4C). Under the optimized conditions (50 mM Tris-HCl [pH 7.5], 100 mM NaCl, 50 μM EDTA, 0.02% [wt/vol] DDM, and an ascorbate-TMPD ratio of 3:1), a nonlinear dependence of the enzyme activity on the concentration of TMPD was observed (Fig. 4D). At a high concentration of TMPD (4 mM), the highest steady-state turnover rate of wild-type Cbb_3-1 was measured to be 2,000 electrons s^{-1}. Although a saturation plateau was not reached, the rates of oxygen reduction catalyzed by *cbb*$_3$-C*c*O still followed Michaelis-Menten kinetics. A Lineweaver-Burk plot of the reciprocals of the initial rates against the reciprocals of the TMPD concentrations was linear (with an R^2 value of 0.991). V_{max} and K_m values were estimated to be 3,978 electrons s^{-1} and 3.6 mM, respectively. We next compared the oxygen reductase activities of both recombinant *cbb*$_3$ isoforms with the wild-type Cbb_3-1. As shown in Fig. 5A, a turnover number of 700 to 800 electrons s^{-1}, which is slightly lower than that found for wild-type Cbb_3-1, was measured for both recombinant *cbb*$_3$ isoforms using 1 mM TMPD.

In addition, we measured the catalase side reaction of *cbb*$_3$-C*c*O in which hydrogen peroxide is decomposed into H_2O and O_2. This catalase activity was originally found in an A-type cytochrome *c* oxidase, the *aa*$_3$-C*c*O from bovine heart (40), and was measured as described for *aa*$_3$-C*c*O from *P. denitrificans* (35) using 600 μM hydrogen peroxide and 500 nM *cbb*$_3$-C*c*O. The catalase activity analysis shows no significant difference, neither between wild-type and recombinant Cbb_3-1 nor between recombinant Cbb_3-1 and Cbb_3-2 (Fig. 5B). Furthermore, the observed catalase activity of *cbb*$_3$-C*c*O (1.6 to 2.4 O_2 min^{-1}) is similar to that of the wild-type *aa*$_3$-C*c*O from *P. denitrificans*.

DISCUSSION

Two *P. stutzeri cbb*$_3$ isoforms are individually isolated based on a newly established homologous expression system. To isolate two *cbb*$_3$ isoforms separately, two different methods might be used: (i) direct isolation of the individual wild-type *cbb*$_3$ isoform from the corresponding *cbb*$_3$ deletion strains, namely, isolation of Cbb_3-1 from the *P. stutzeri* ΔCbb_3-2 strain and of Cbb_3-2 from the ΔCbb_3-1 strain; (ii) production of both *cbb*$_3$ isoforms by using a combination of expression vectors and deletion strains. However, the first method was not applicable for *P. stutzeri* because the expression of both isoenzymes seems to be interdependent. Cbb_3-2 was not detectable in *P. stutzeri* membranes when the operon *ccoNOP-1* was deleted from the genome. Furthermore, if the operon *ccoNOQP*-2 was deleted, the amount of Cbb_3-1 was also drastically decreased (data not shown). Because of a lack of experimental evidence, we cannot propose a straightforward explanation for this observation. Therefore, the second method had to be followed.

We constructed two expression vectors, each containing either one of the two *cbb*$_3$ operons, in addition specifying also a Strep tag II fused to the C terminus of the CcoN subunit. For complementation, the expression vectors were transformed into the respective *P. stutzeri* deletion strains. Now both *cbb*$_3$ operons were present again in the same strain, which has one *cbb*$_3$ operon in the genome and the other one on the expression vector. Two *cbb*$_3$ isoforms are expressed, and both *cbb*$_3$ isoforms can be easily purified from the respective strains by affinity purification. The purity of both isolated isoforms was confirmed by SDS- and BN-PAGE analyses and peptide mass fingerprinting analysis. Furthermore, this newly established expression system enables us not only to produce and isolate both *cbb*$_3$ isoforms separately but also to genetically manipulate both *cbb*$_3$ isoforms for future functional studies, i.e., by site-directed mutagenesis.

Expression of the two *cbb*$_3$ isoforms is regulated at the transcriptional level in response to the peripheral oxygen concentration. DNA sequence analysis revealed that the promoters of the two *cbb*$_3$ operons contain different regulatory elements (Fig. 6). Both promoters (P1 and P2) contain the putative sigma factor

RpoD (σ^{70}) binding site (−35 and −10 regions), while only the P1 promoter possesses a consensus binding site for the transcription activator ANR (a homologue of *E. coli* FNR), which is centered at position −95.5 relative to the start codon of *ccoN*-1 and overlaps with the −35 region by one base pair. Such overlapping is a typical feature of the ANR/FNR-dependent promoters and allows the activation of transcription by direct interaction with the RNA polymerase (41, 42). In the genomes of *P. aeruginosa* and *P. putida*, which both contain two cbb_3 operons, also only one of the operons is preceded by an ANR binding site in its promoter region (28, 43). Moreover, we found that the organization of the ANR binding site and −35 promoter elements in *P. stutzeri* are similar to those published previously for *P. putida* (43).

For the cbb_3-C*c*Os, ANR has been reported to function as a positive regulator of gene expression in response to oxygen limitation (28, 29, 43–45). In *P. aeruginosa*, the expression pattern and regulation of the two cbb_3 isoforms under different growth conditions were already investigated in detail (28, 29). It has been shown that the expression of *P. aeruginosa* Cbb_3-2 (corresponding to *P. stutzeri* Cbb_3-1) from its ANR-dependent promoter is highly dependent on the oxygen concentration in the environment and is dramatically upregulated under low-oxygen conditions or in the stationary phase. The induction of *P. aeruginosa* Cbb_3-2 in the latter case was also suggested to be the result of an excessive oxygen consumption due to the high cell density (46). In contrast, the genes for *P. aeruginosa* Cbb_3-1 (corresponding to Cbb_3-2 of *P. stutzeri*) are constitutively expressed under regulation of an ANR-independent cbb_3 promoter, and its expression is not directly correlated to the different levels of oxygen or certain growth phases (28, 29).

In this study, we found that under microaerobic growth conditions, the yield of pure Cbb_3-1 was 6- to 8-fold higher than that of Cbb_3-2 if the proteins were expressed under the control of their native promoters in the recombinant *P. stutzeri* strains (see Table 2). This result is consistent with the previously reported finding that the ANR-dependent cbb_3 promoter in *P. aeruginosa* showed an 8-fold-higher activity than the ANR-independent one under low oxygen concentrations (29). Additionally, our results also show that the yield of recombinant Cbb_3-2 can be increased to the same level as Cbb_3-1 when its native ANR-independent promoter P2 is replaced by the ANR-dependent promoter P1 (Table 2). In good agreement with the literature (28, 29), our results indicate that the expression of Cbb_3-1 (*P. stutzeri* nomenclature) is regulated by the environmental oxygen concentration and that this isoform plays a primary role under oxygen-limited conditions. Supposedly, the different expression patterns of the two cbb_3 isoforms could reflect their different affinities for oxygen, which will be addressed in future investigations.

Both cbb_3-C*c*Os from *P. stutzeri* show high oxygen reductase activity using TMPD as the electron donor. Because very little is known about the native electron donors of *P. stutzeri* cbb_3-C*c*O, an artificial electron-donating system consisting of TMPD and ascorbate was used for the functional analysis of cbb_3-C*c*Os. As a substrate, TMPD can directly donate electrons to cbb_3-C*c*O, while ascorbate maintains TMPD in the reduced state. Under conditions optimized for pH, ionic strength, and the molar ratio of ascorbate to TMPD, we showed that the purified recombinant Cbb_3-1 and Cbb_3-2 catalyze the reduction of oxygen at a rate comparable to the wild-type Cbb_3-1 (Fig. 5A). This observation suggests that the recombinant proteins produced in our newly established expression system are fully active. We found that the oxygen reductase activity of cbb_3-C*c*O increased with increasing concentrations of TMPD up to a maximum at 4 mM (Fig. 4D). At 0.5 mM TMPD, the enzymatic activity of 450 electrons s^{-1} is compatible with the activities of 200 to 600 electrons s^{-1} measured for the purified cbb_3-C*c*O from *R. sphaeroides* under the same conditions (17, 47, 48). Moreover, our values of 700 to 800 electrons s^{-1} determined at 1 mM TMPD are in good agreement with the values previously reported for the *P. stutzeri* cbb_3-C*c*O using the same TMPD concentration (16, 30). However, we found that the oxygen reductase activity of cbb_3-C*c*O is not saturated at 1 mM TMPD. With an increased TMPD concentration of 4 mM, a rate of about 2,000 electrons s^{-1} was determined (Fig. 4D). Although the activity displayed Michaelis-Menten kinetics for the TMPD substrate, a saturation plateau was still not attained due to two technical difficulties in using a concentration of TMPD above 4 mM. First, it was difficult to maintain the pH of the reaction buffer at 7.5 (the optimal pH for cbb_3-C*c*O) because the addition of large amounts of TMPD and ascorbate led to a substantial decrease in pH. Second, at high concentrations of TMPD, a relatively high level of TMPD autoxidation caused a significant decrease of the oxygen concentration, which resulted in a very long equilibrium time before the reaction could be initiated.

We could calculate two apparent kinetic parameters (a K_m of 3.6 mM and a V_{max} of about 4,000 electrons s^{-1}). Both values, obtained in the absence of well-defined saturation, are unusually high and may not represent true kinetic constants. Nevertheless, we can safely conclude that the *P. stutzeri* cbb_3-C*c*Os can catalyze the reduction of oxygen at a rate of at least 2,000 electrons s^{-1} *in vitro* and that the K_m for TMPD must be higher than 1 mM. Although a high turnover number of greater than 900 electrons s^{-1} has also been reported for the *R. sphaeroides* cbb_3-C*c*O (49), these kinetic features do not seem to apply to other cbb_3-C*c*Os, because kinetic studies on the *H. pylori* cbb_3-C*c*O showed a very high affinity for TMPD (K_m = 108 μM) but a relatively low V_{max} (247 electrons s^{-1}) (50). It has to be noted that in the case of the *H. pylori* cbb_3-C*c*O, the catalytic activity was measured by monitoring the pH shift with sodium ascorbate as the ultimate electron donor (50, 51), which excludes a direct comparison between our results and those from the *H. pylori* cbb_3-C*c*O. In the caa_3-C*c*O, a member of the A2 subclass of the A-type HCOs (4), subunit II, contains a single *c*-type heme, which can directly receive the electrons from TMPD. Interestingly, it has been shown for the caa_3-C*c*O of *Bacillus subtilis* that a high level of TMPD (at least 5 mM) is also required to reach the maximal activity of caa_3-C*c*O (52).

The oxygen reductase activities of aa_3-C*c*Os are normally in the range of 400 to 600 electrons s^{-1} (53), which is about 4-fold lower than the highest activity (2,000 electrons s^{-1}) observed for cbb_3-C*c*O in this study. In the case of aa_3-C*c*O, TMPD functions only as a redox mediator between the mobile cytochrome *c* and the Cu_A-containing subunit II of aa_3-C*c*O. The formation and dissociation of a complex between cytochrome *c* and aa_3-C*c*O are required for the electron transfer to occur (1, 54), which may represent a rate-limiting step in the overall reaction and result in a less efficient electron transfer compared to cbb_3-C*c*O. In contrast, the presence of three *c*-type cytochromes in the subunit CcoO and CcoP of the cbb_3-C*c*Os may provide multiple electron entry sites and support simultaneous interactions between TMPD and cbb_3-C*c*Os. As confirmed by the cbb_3-C*c*O structure (19), the edge-to-edge distances from heme *c* of CcoO to heme *b* and from heme *b* to heme

b_3 are clearly shorter than the distances observed for the corresponding redox centers in aa_3-C*c*O. As previously suggested (19, 55), the shorter distances may accelerate the rates of electron transfer and could potentially increase the trapping efficiency of O_2. All of these features led us to propose that electron transfer in the cbb_3-C*c*Os is more efficient than that in aa_3-C*c*Os under these *in vitro* assay conditions.

Comparison of the oxygen reductase activity of the two isoforms Cbb_3-1 and Cbb_3-2, however, revealed only marginal differences, which may be due to the fact that an artificial electron donor was used, which has a high efficiency for both cbb_3 isoforms. A different picture may evolve if a specific endogenous electron donor for the isoforms is available for activity assays. Inferring from the amino acid sequences and a surface charge calculation based on the X-ray structure of Cbb_3-1 as well as a model of Cbb_3-2, we would expect the most pronounced structural changes and surface charge differences to occur in the solvent exposed domains of subunits CcoP-1 and CcoP-2, which may constitute the putative cytochrome *c* binding site with the respective electron entry area. These findings give rise to the hypothesis that two cbb_3 isoforms may differ with respect to their physiological substrate. Therefore, our future interest will focus on the identification of the endogenous electron donor as well as proton pumping characteristics and potential differences of the two cbb_3 isoforms.

The two cbb_3 isoforms possess similar biochemical and biophysical properties but different subunit composition and stability. The results reported in this work show that the two isoforms of cbb_3-C*c*Os of *P. stutzeri* share high levels of similarity in their biochemical and biophysical properties, including oxygen reductase and catalase activities as well as spectral properties. A remarkable difference between both cbb_3 isoforms is the subunit composition concerning the presence/absence of the CcoQ subunit. Our peptide mass fingerprinting analysis revealed that CcoQ is associated only with Cbb_3-2, which is in line with the observations that the *ccoQ* gene is found only in the second *ccoNOQP*-2 operon and that this gene product does not associate with the Cbb_3-1 complex as has already been documented by its X-ray structure (19).

The physiological role of CcoQ in cbb_3-C*c*Os is still under debate. In *Bradyrhizobium japonicum* and *R. sphaeroides*, it was shown that deletion of CcoQ had no effect on assembly or catalytic activity of cbb_3-C*c*O (22, 56). In contrast, the activity of *R. capsulatus* cbb_3-C*c*O was significantly reduced in the absence of CcoQ (23). Additionally, it has been demonstrated that CcoQ is required to protect the *R. sphaeroides* cbb_3-C*c*O from degradation under aerobic conditions (24). The absence of CcoQ in the *P. stutzeri* Cbb_3-1 may be a consequence of the fact that this isoform is expressed mainly at very low oxygen tensions, i.e., CcoQ is not required to protect the core complex from the oxygen-induced instability and degradation.

In addition, our DSC results show that Cbb_3-1 is more stable than Cbb_3-2. The total calorimetric enthalpy changes of the recombinant Cbb_3-1 and Cbb_3-2 are 2,016 and 1,556 KJ mol^{-1}, respectively. Both values are similar to the reported value of 1,560 KJ mol^{-1} for the aa_3-C*c*O from *P. denitrificans* (37). The DSC scan of aa_3-C*c*O showed two transition peaks. The low-temperature transition centered at 48°C was assigned to the denaturation of subunit III of aa_3-C*c*O, while subunit I and II denatures as a single cooperative unit at 68°C (37). In the case of cbb_3-C*c*O, two transition peaks can also be identified, although they are not as well separated as observed for Cbb_3-2. Based on the observation that two assembly intermediates are present in cbb_3-C*c*O (9, 21), we hypothesize that the low-temperature peak corresponds to the thermal denaturation of subunit CcoP, whereas the second peak is caused by denaturation of subunits CcoN and CcoO. In addition, besides the presence of CcoQ in Cbb_3-2, small structural differences may lead to the difference in thermal stability between Cbb_3-1 and Cbb_3-2.

In summary, we successfully established a homologous expression system that enables us to isolate both cbb_3 isoforms individually. The two purified cbb_3 isoforms from *P. stutzeri* share a high degree of similarity in terms of their biochemical and biophysical properties. On the other hand, differences were observed in respect to subunit composition, thermal stability, and regulation of both cbb_3-C*c*Os. Finally, the present work will serve as a suitable platform for future functional and structural studies on the two isoforms of cbb_3-C*c*O, in particular of the investigation of proton pumping capacities and of their physiological substrates.

ACKNOWLEDGMENTS

We thank Hannelore Müller, Cornelia Münke, and Imke Wüllenweber for excellent technical assistance and Oliver-Matthias H. Richter (Goethe University) for advice concerning the construction of deletion strains and expression vectors. We are very grateful to Iris von der Hocht (Jülich Research Centre), Florian Hilbers (Aarhus University), and Martin Kohlstädt for insightful discussions.

This work was supported by the Max Planck Society and the Cluster of Excellence "Macromolecular Complexes" Frankfurt.

REFERENCES

1. **Richter O, Ludwig B.** 2009. Electron transfer and energy transduction in the terminal part of the respiratory chain—lessons from bacterial model systems. Biochim. Biophys. Acta **1787:**626–634. http://dx.doi.org/10.1016/j.bbabio.2009.02.020.
2. **Hosler JP, Ferguson-Miller S, Mills DA.** 2006. Energy transduction: proton transfer through the respiratory complexes. Annu. Rev. Biochem. **75:**165–187. http://dx.doi.org/10.1146/annurev.biochem.75.062003.101730.
3. **Yoshikawa S, Muramoto K, Shinzawa-Itoh K.** 2011. Proton-pumping mechanism of cytochrome *c* oxidase. Annu. Rev. Biophys. **40:**205–223. http://dx.doi.org/10.1146/annurev-biophys-042910-155341.
4. **Pereira M, Santana M, Teixeira M.** 2001. A novel scenario for the evolution of haem-copper oxygen reductases. Biochim. Biophys. Acta **1505:**185–208. http://dx.doi.org/10.1016/S0005-2728(01)00169-4.
5. **Sousa FL, Alves RJ, Ribeiro MA, Pereira-Leal JB, Teixeira M, Pereira MM.** 2012. The superfamily of heme-copper oxygen reductases: types and evolutionary considerations. Biochim. Biophys. Acta **1817:**629–637. http://dx.doi.org/10.1016/j.bbabio.2011.09.020.
6. **Ducluzeau A, Ouchane S, Nitschke W.** 2008. The cbb_3 oxidases are an ancient innovation of the domain bacteria. Mol. Biol. Evol. **25:**1158–1166. http://dx.doi.org/10.1093/molbev/msn062.
7. **Cosseau C, Batut J.** 2004. Genomics of the *ccoNOQP*-encoded cbb_3 oxidase complex in bacteria. Arch. Microbiol. **181:**89–96. http://dx.doi.org/10.1007/s00203-003-0641-5.
8. **Pitcher R, Watmough N.** 2004. The bacterial cytochrome cbb_3 oxidases. Biochim. Biophys. Acta **1655:**388–399. http://dx.doi.org/10.1016/j.bbabio.2003.09.017.
9. **Ekici S, Pawlik G, Lohmeyer E, Koch H-G, Daldal F.** 2011. Biogenesis of cbb_3-type cytochrome *c* oxidase in *Rhodobacter capsulatus*. Biochim. Biophys. Acta **3:**pii=e00293-11. http://dx.doi.org/10.1128/mBio.00293-11.
10. **Pitcher R, Brittain T, Watmough N.** 2002. Cytochrome cbb_3 oxidase and bacterial microaerobic metabolism. Biochem. Soc. Trans. **30:**653–658.
11. **Preisig O, Zufferey R, Thöny-Meyer L, Appleby CA, Hennecke H.** 1996. A high-affinity cbb_3-type cytochrome oxidase terminates the symbiosis-specific respiratory chain of *Bradyrhizobium japonicum*. J. Bacteriol. **178:**1532–1538.
12. **Arslan E, Kannt A, Thöny-Meyer L, Hennecke H.** 2000. The symbiotically essential cbb_3-type oxidase of *Bradyrhizobium japonicum* is a proton pump. FEBS Lett. **470:**7–10. http://dx.doi.org/10.1016/S0014-5793(00)01277-1.

13. **Smith MA, Finel M, Korolik V, Mendz GL.** 2000. Characteristics of the aerobic respiratory chains of the microaerophiles *Campylobacter jejuni* and *Helicobacter pylori*. Arch. Microbiol. **174:**1–10. http://dx.doi.org/10.1007/s002030000174.
14. **Deeudom M, Rock J, Moir J.** 2006. Organization of the respiratory chain of *Neisseria meningitidis*. Biochem. Soc. Trans. **34:**139–142. http://dx.doi.org/10.1042/BST0340139.
15. **Hino T, Matsumoto Y, Nagano S, Sugimoto H, Fukumori Y, Murata T, Iwata S, Shiro Y.** 2010. Structural basis of biological N_2O generation by bacterial nitric oxide reductase. Science **330:**1666–1670. http://dx.doi.org/10.1126/science.1195591.
16. **Forte E, Urbani A, Saraste M, Sarti P, Brunori M, Giuffrè A.** 2001. The cytochrome cbb_3 from *Pseudomonas stutzeri* displays nitric oxide reductase activity. Eur. J. Biochem. **268:**6486–6491. http://dx.doi.org/10.1046/j.0014-2956.2001.02597.x.
17. **Huang Y, Reimann J, Lepp H, Drici N, Adelroth P.** 2008. Vectorial proton transfer coupled to reduction of O_2 and NO by a heme-copper oxidase. Proc. Natl. Acad. Sci. U. S. A. **105:**20257–20262. http://dx.doi.org/10.1073/pnas.0805429106.
18. **Giuffre A, Stubauer G, Sarti P, Brunori M, Zumft W, Buse G, Soulimane T.** 1999. The heme-copper oxidases of *Thermus thermophilus* catalyze the reduction of nitric oxide: evolutionary implications. Proc. Natl. Acad. Sci. U. S. A. **96:**14718–14723. http://dx.doi.org/10.1073/pnas.96.26.14718.
19. **Buschmann S, Warkentin E, Xie H, Langer J, Ermler U, Michel H.** 2010. The structure of cbb_3 cytochrome oxidase provides insights into proton pumping. Science **329:**327–330. http://dx.doi.org/10.1126/science.1187303.
20. **Preisig O, Anthamatten D, Hennecke H.** 1993. Genes for a microaerobically induced oxidase complex in *Bradyrhizobium japonicum* are essential for a nitrogen-fixing endosymbiosis. Proc. Natl. Acad. Sci. U. S. A. **90:**3309–3313. http://dx.doi.org/10.1073/pnas.90.8.3309.
21. **Kulajta C, Thumfart J, Haid S, Daldal F, Koch H.** 2006. Multi-step assembly pathway of the cbb_3-type cytochrome *c* oxidase complex. J. Mol. Biol. **355:**989–1004. http://dx.doi.org/10.1016/j.jmb.2005.11.039.
22. **Zufferey R, Preisig O, Hennecke H, Thöny-Meyer L.** 1996. Assembly and function of the cytochrome cbb_3 oxidase subunits in *Bradyrhizobium japonicum*. J. Biol. Chem. **271:**9114–9119. http://dx.doi.org/10.1074/jbc.271.15.9114.
23. **Peters A, Kulajta C, Pawlik G, Daldal F, Koch H.** 2008. Stability of the cbb_3-type cytochrome oxidase requires specific CcoQ-CcoP interactions. J. Bacteriol. **190:**5576–5586. http://dx.doi.org/10.1128/JB.00534-08.
24. **Oh J, Kaplan S.** 2002. Oxygen adaptation. The role of the CcoQ subunit of the cbb_3 cytochrome *c* oxidase of *Rhodobacter sphaeroides* 2.4.1. J. Biol. Chem. **277:**16220–16228. http://dx.doi.org/10.1074/jbc.M200198200.
25. **Lalucat J, Bennasar A, Bosch R, Garcia-Valdes E, Palleroni N.** 2006. Biology of *Pseudomonas stutzeri*. Microbiol. Mol. Biol. Rev. **70:**510–547. http://dx.doi.org/10.1128/MMBR.00047-05.
26. **Pitcher R, Cheesman M, Watmough N.** 2002. Molecular and spectroscopic analysis of the cytochrome cbb_3 oxidase from *Pseudomonas stutzeri*. J. Biol. Chem. **277:**31474–31483. http://dx.doi.org/10.1074/jbc.M204103200.
27. **Peña A, Busquets A, Gomila M, Bosch R, Nogales B, García-Valdés E, Lalucat J, Bennasar A.** 2012. Draft genome of *Pseudomonas stutzeri* strain ZoBell (CCUG 16156), a marine isolate and model organism for denitrification studies. J. Bacteriol. **194:**1277–1278. http://dx.doi.org/10.1128/JB.06648-11.
28. **Comolli J, Donohue T.** 2004. Differences in two *Pseudomonas aeruginosa* cbb_3 cytochrome oxidases. Mol. Microbiol. **51:**1193–1203. http://dx.doi.org/10.1046/j.1365-2958.2003.03904.x.
29. **Kawakami T, Kuroki M, Ishii M, Igarashi Y, Arai H.** 2010. Differential expression of multiple terminal oxidases for aerobic respiration in *Pseudomonas aeruginosa*. Environ. Microbiol. **12:**1399–1412. http://dx.doi.org/10.1111/j.1462-2920.2009.02109.x.
30. **Urbani A, Gemeinhardt S, Warne A, Saraste M.** 2001. Properties of the detergent solubilised cytochrome *c* oxidase (cytochrome cbb_3) purified from *Pseudomonas stutzeri*. FEBS Lett. **508:**29–35. http://dx.doi.org/10.1016/S0014-5793(01)03006-X.
31. **Choi K, Kumar A, Schweizer H.** 2006. A 10-min method for preparation of highly electrocompetent *Pseudomonas aeruginosa* cells: application for DNA fragment transfer between chromosomes and plasmid transformation. J. Microbiol. Methods **64:**391–397. http://dx.doi.org/10.1016/j.mimet.2005.06.001.
32. **Laemmli UK.** 1970. Cleavage of structural proteins during the assembly of the head of bacteriophage T4. Nature **227:**680–685. http://dx.doi.org/10.1038/227680a0.
33. **Thomas PE, Ryan D, Levin W.** 1976. An improved staining procedure for the detection of the peroxidase activity of cytochrome P-450 on sodium dodecyl sulfate polyacrylamide gels. Anal. Biochem. **75:**168–176. http://dx.doi.org/10.1016/0003-2697(76)90067-1.
34. **Schagger H, von Jagow G.** 1991. Blue native electrophoresis for isolation of membrane protein complexes in enzymatically active form. Anal. Biochem. **199:**223–231. http://dx.doi.org/10.1016/0003-2697(91)90094-A.
35. **Hilbers F, von der Hocht I, Ludwig B, Michel H.** 2013. True wild type and recombinant wild type cytochrome *c* oxidase from *Paracoccus denitrificans* show a 20-fold difference in their catalase activity. Biochim. Biophys. Acta **1827:**319–327. http://dx.doi.org/10.1016/j.bbabio.2012.10.008.
36. **Yan Y, Yang J, Dou Y, Chen M, Ping S, Peng J, Lu W, Zhang W, Yao Z, Li H, Liu W, He S, Geng L, Zhang X, Yang F, Yu H, Zhan Y, Li D, Lin Z, Wang Y, Elmerich C, Lin M, Jin Q.** 2008. Nitrogen fixation island and rhizosphere competence traits in the genome of root-associated *Pseudomonas stutzeri* A1501. Proc. Natl. Acad. Sci. U. S. A. **105:**7564–7569. http://dx.doi.org/10.1073/pnas.0801093105.
37. **Haltia T, Semo N, Arrondo J, Goni F, Freire E.** 1994. Thermodynamic and structural stability of cytochrome *c* oxidase from *Paracoccus denitrificans*. Biochemistry **33:**9731–9740. http://dx.doi.org/10.1021/bi00198a044.
38. **Morin PE, Diggs D, Freire E.** 1990. Thermal stability of membrane-reconstituted yeast cytochrome *c* oxidase. Biochemistry **29:**781–788. http://dx.doi.org/10.1021/bi00455a028.
39. **Manetto GD, La Rosa C, Grasso DM, Milardi D.** 2005. Evaluation of thermodynamic properties of irreversible protein thermal unfolding measured by DSC. J. Therm. Anal. Calorim. **80:**263–270. http://dx.doi.org/10.1007/s10973-005-0646-1.
40. **Orii Y, Okunuki K.** 1963. Studies on cytochrome *a*. X. Effect of hydrogen peroxide on absorption spectra of cytochrome *a*. J. Biochem. **54:**207–213.
41. **Körner H, Sofia HJ, Zumft WG.** 2003. Phylogeny of the bacterial superfamily of Crp-Fnr transcription regulators: exploiting the metabolic spectrum by controlling alternative gene programs. FEMS Microbiol. Rev. **27:**559–592. http://dx.doi.org/10.1016/S0168-6445(03)00066-4.
42. **Wing HJ, Green J, Guest JR, Busby SJ.** 2000. Role of activating region 1 of *Escherichia coli* FNR protein in transcription activation at class II promoters. J. Biol. Chem. **275:**29061–29065. http://dx.doi.org/10.1074/jbc.M000390200.
43. **Ugidos A, Morales G, Rial E, Williams HD, Rojo F.** 2008. The coordinate regulation of multiple terminal oxidases by the *Pseudomonas putida* ANR global regulator. Environ. Microbiol. **10:**1690–1702. http://dx.doi.org/10.1111/j.1462-2920.2008.01586.x.
44. **Swem DL, Bauer CE.** 2002. Coordination of ubiquinol oxidase and cytochrome cbb_3 oxidase expression by multiple regulators in *Rhodobacter capsulatus*. J. Bacteriol. **184:**2815–2820. http://dx.doi.org/10.1128/JB.184.10.2815-2820.2002.
45. **Mouncey NJ, Kaplan S.** 1998. Oxygen regulation of the *ccoN* gene encoding a component of the cbb_3 oxidase in *Rhodobacter sphaeroides* 2.4.1T: involvement of the FnrL protein. J. Bacteriol. **180:**2228–2231.
46. **Arai H.** 2011. Regulation and function of versatile aerobic and anaerobic respiratory metabolism in *Pseudomonas aeruginosa*. Front. Microbiol. **2:**103. http://dx.doi.org/10.3389/fmicb.2011.00103.
47. **Lee HJ, Gennis RB, Adelroth P.** 2011. Entrance of the proton pathway in cbb_3-type heme-copper oxidases. Proc. Natl. Acad. Sci. U. S. A. **108:**17661–17666. http://dx.doi.org/10.1073/pnas.1107543108.
48. **Sharma V, Puustinen A, Wikstrom M, Laakkonen L.** 2006. Sequence analysis of the cbb_3 oxidases and an atomic model for the *Rhodobacter sphaeroides* enzyme. Biochemistry **45:**5754–5765. http://dx.doi.org/10.1021/bi060169a.
49. **García-Horsman JA, Berry E, Shapleigh JP, Alben JO, Gennis RB.** 1994. A novel cytochrome *c* oxidase from *Rhodobacter sphaeroides* that lacks Cu_A. Biochemistry **33:**3113–3119. http://dx.doi.org/10.1021/bi00176a046.
50. **Tsukita S, Koyanagi S, Nagata K, Koizuka H, Akashi H, Shimoyama T, Tamura T, Sone N.** 1999. Characterization of a *cb*-type cytochrome *c* oxidase from *Helicobacter pylori*. J. Biochem. **125:**194–201. http://dx.doi.org/10.1093/oxfordjournals.jbchem.a022259.
51. **Nagata K, Tsukita S, Tamura T, Sone N.** 1996. A *cb*-type cytochrome-*c* oxidase terminates the respiratory chain in *Helicobacter pylori*. Microbiology **142**(Part 7):1757–1763.
52. **Assempour M, Lim D, Hill BC.** 1998. Electron transfer kinetics during the reduction and turnover of the cytochrome caa_3 complex from *Bacillus subtilis*. Biochemistry **37:**9991–9998. http://dx.doi.org/10.1021/bi980331c.
53. **Dürr K, Koepke J, Hellwig P, Muller H, Angerer H, Peng G, Olkhova**

E, Richter O, Ludwig B, Michel H. 2008. A D-pathway mutation decouples the *Paracoccus denitrificans* cytochrome *c* oxidase by altering the side-chain orientation of a distant conserved glutamate. J. Mol. Biol. **384:** 865–877. http://dx.doi.org/10.1016/j.jmb.2008.09.074.

54. **Maneg O, Malatesta F, Ludwig B, Drosou V.** 2004. Interaction of cytochrome *c* with cytochrome oxidase: two different docking scenarios. Biochim. Biophys. Acta **1655:**274–281. http://dx.doi.org/10.1016/j.bbabio.2003.10.010.
55. **Verkhovsky MI, Morgan JE, Puustinen A, Wikstrom M.** 1996. Kinetic trapping of oxygen in cell respiration. Nature **380:**268–270. http://dx.doi.org/10.1038/380268a0.
56. **Oh JI, Kaplan S.** 1999. The cbb_3 terminal oxidase of *Rhodobacter sphaeroides* 2.4.1: structural and functional implications for the regulation of spectral complex formation. Biochemistry **38:**2688–2696. http://dx.doi.org/10.1021/bi9825100.
57. **ZoBell CE, Upham HC.** 1944. A list of marine bacteria including descriptions of sixty new species. Bull. Scripps Inst. Oceanogr. **5:**239–292.
58. **Kovach M, Phillips R, Elzer P, Roop R, Peterson K.** 1994. pBBR1MCS: a broad-host-range cloning vector. Biotechniques **16:**800–802.
59. **Kovach M, Elzer P, Hill D, Robertson G, Farris M, Roop R, Peterson K.** 1995. Four new derivatives of the broad-host-range cloning vector pBBR1MCS, carrying different antibiotic-resistance cassettes. Gene **166:** 175–176. http://dx.doi.org/10.1016/0378-1119(95)00584-1.